SCIENCE CHINA
Technological Sciences

December 2011 Vol.54 No.12: 3243–3250
doi: 10.1007/s11431-011-4622-7

Free return orbit design and characteristics analysis for manned lunar mission

PENG QiBo, SHEN HongXin & LI HaiYang*

College of Aerospace and Material Engineering, National Univ. of Defense Technology, Changsha 410073, China

Received February 23, 2011; accepted June 12, 2011; published online November 5, 2011

A circumlunar free return orbit design model that satisfies manned lunar mission constraints is established. By combining analytical method with numerical method, a serial orbit design strategy from initial value design to precision solution is proposed. A simulation example is given, and the conclusion indicates that the method has excellent convergence performance and precision. According to a great deal of simulation results solved by the method, the free return orbit characters such as accessible moon orbit parameters, return orbit parameters, transfer delta velocity, etc. are analyzed, which can supply references to constitute manned lunar mission orbit scheme.

manned lunar mission, free return orbit, orbit design, orbit characters

Citation: Peng Q B, Shen H X, Li H Y. Free return orbit design and characteristics analysis for manned lunar mission. Sci China Tech Sci, 2011, 54: 3243–3250, doi: 10.1007/s11431-011-4622-7

1 Introduction

In January 2004, president George W. Bush announced a new vision for space exploration–Constellation Program for the National Aeronautics and Space Administration (NASA) that would return humans to the Moon by 2020, but later this mission was cancelled by Barack H. Obama. However, with NASA's Constellation Program putting forward, many countries began to pay their attention to manned lunar mission, and more researches on this were reported. Trans-lunar orbit design, which is one of the study contents for manned lunar mission, performs a key function for safely landing a spacecraft on the moon. Different from unmanned lunar exploration, the safety of astronauts is always of dominant importance, and the abort capability must be considered in orbit design. Although the abort is usually not carried out, the design of abort orbit is as important as the normal mission orbit, especially in the sense of ensuring the safety of astronauts. A circumlunar free return orbit (FRO), in which the spacecraft can return to earth without orbit maneuvers when an emergency occurs, is very significant to lunar abort mission, so it is widely used in manned lunar missions. But before using FRO as an orbit for manned lunar mission, its design method and orbit characteristics should be studied first.

By now, only the Apollo program has sent the men on the moon successfully. Many analysis of FRO were done in the Apollo mission [1–6]. But the design method and computation capability in the Apollo era were quite different from now, and the studies were mainly focused on the mission analysis, the detailed design models and methods were not given in the references. Recently, some researchers have made effort in FRO study for new manned lunar landing mission. Ref. [4] gave the description of FRO and brief characteristics. Refs. [5, 6] proposed a FRO design method based on the double two-body model, but the precision was limited. Refs. [7–9] designed more accurate FROs using different methods, but due to the complexity, these methods can not be used for ex-

*Corresponding author (email: poochie003@163.com)

tensive simulations.

Meanwhile, some researchers employed optimization algorithm for orbit design and obtained good results [10]. Following this research, a systematic study of optimization design of FRO is presented in this paper. Firstly, the circumlunar FRO design model that satisfies manned lunar mission constraints is established. Then, by combining analytical method with numerical method, a serial orbit design strategy from initial value design to accurate solution is proposed. The solution indicates that the method has good convergence performance and precision. Based on this, the FRO characters such as accessible moon orbit parameters, return orbit parameters and transfer velocity are analyzed detailedly based on a great deal of simulations, which can supply references to manned lunar mission design.

2 Problem statement

2.1 Free return orbit

A FRO lunar transfer is characterized by its zero delta velocity (Δv) requirements for return to earth. In this orbit, once the trans-lunar injection (TLI) burn is initiated in the low earth orbit (LEO), the spacecraft will slingshot around the moon and return to proper reentry interface with only small orbit correction. This subset of lunar orbit is utilized such that in the event of an engine failure or other type of emergency, the spacecraft will still return to earth. So the motivation for using it for manned lunar mission is apparent. The FRO was utilized for Apollo 8, Apollo 10, Apollo 11 and Apollo 12 missions. In addition, the FRO also can be used as an abort orbit for manned lunar mission as in Apollo 13. For safety's sake, FRO is utmost important for manned lunar mission.

The flight profile utilizing FRO can be described as follows. Firstly, the spacecraft is injected to trans-lunar orbit from LEO. When it reaches the perilune *C*, a lunar orbit injection (LOI) delta velocity is acquired, and the spacecraft is sent to the low lunar orbit (LLO). If an emergency occurs in trans-lunar flight, the lunar orbit injection burn would be cancelled and the spacecraft would fly around the moon and return to the earth. The flight profile is shown in Figure 1.

2.2 Coordinate systems

The following coordinate systems are established for the FRO design.

1) Earth centered inertial (ECI) coordinate system O_E-XYZ.

The origin is at the center of the earth, the axis X is pointing toward the vernal equinox, the Z axis is along the earth's polar axis of rotation.

2) Moon centered inertial (MCI) coordinate system O_L-xyz.

The origin is at the center of the moon, the xy plane of the reference frame is the moon's orbit plane at time t_0, the x axis is along the direction from the center of the earth to the moon, the z axis is along the normal direction of the moon' orbit plane.

3) Moon centered fixed (MCF) coordinate system $O_L - x'y'z'$.

The origin is at the center of the moon, the x' axis is in the moon's equator plane, pointing toward the Sinus-Medii, the z' axis is along the moon's polar axis of rotation.

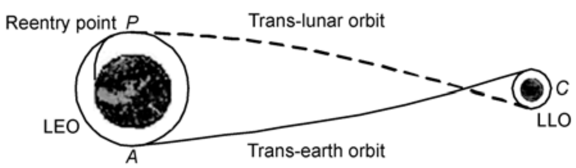

Figure 1 Schematic figure of free return orbit.

3 FRO design method

According to the precision requirements, different models will be used for orbit design, which include the two body model, double two-body model, restricted three-body model, high precision dynamics model, etc. [11, 12].

In this paper, the double two-body model and high precision dynamics model are used for the FRO design, in which, the analytic model based on patched-conic method is used for initial design, and the high precision model under various perturbations is used for accurate orbit parameters solution. Both in initial values solution and in accurate values solution, the optimization method is utilized. By using the optimization method, we transform the FRO design to an optimal control problem with constraints to solve. The FRO design strategy is shown in Figure 2. The detailed method for FRO design will be given as follows.

3.1 Initial orbit design

The patched-conic method is a pure algebraic method that

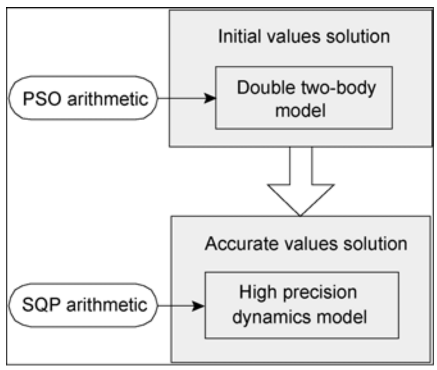

Figure 2 Solution strategy for FRO design.

does not need trajectory integral. Because of the rapid calculation characters, it is suitable for preliminary design of FRO. As the moon is assumed as running around the earth in a circular orbit in double two-body model, the calculation precision is extremely limited. For this, the accurate position and velocity relation between the earth and the moon is considered in the double two-body model by using the ephemeris in the study. In addition, to reduce the search time, the particle swarm optimization (PSO) algorithm is used to improve the computing efficiency. The optimal control problem is formulated in the following.

a) Design variables.

Many orbit parameters can be used as design variables for patched-conic method. In this paper, the following parameters are chosen for design variables, and others orbit parameters can be solved by the design variables.

1) The time T_B when the spacecraft arrives at the entrance point B;

2) The inclination i_E of the spacecraft in LEO;

3) The argument of latitude u_E of the spacecraft at point A in the ECI coordinate system;

4) The longitude λ_B and latitude φ_B of the spacecraft at entrance point B in the MCI coordinate system.

T_B and i_E are the input parameters, and other variables are the search parameters. There are two approaches which are ascent phase arriving and descent phase arriving for FRO design. The design method is the same for both of them, so only the ascent phase arriving approach is presented in the paper.

b) Orbit model.

The double two-body model, which is an approximate of restricted three-body model, is used for initial orbit design. In this model, the trans-lunar orbit is divided into two segments, the earth centered phase and the moon centered phase. The earth gravitation is only considered in the earth centered phase, while the moon gravitation is only be considered in the other. The two conic orbit segments are patched at the boundary of the influence zone of the lunar gravity, and the gravity of sun and other perturbations are ignored [11].

The moon is assumed as running around the earth in a circular orbit within a radius of 384400 km for traditional patched-conic method, and the average velocity of the moon is about 1.018 km/s. Practically, the moon is running in a elliptic orbit with an eccentricity about 0.0549. The maximum error of the earth-moon distance between the traditional double two-body assumption and actual orbit is about 20000 km, and the maximum error of moon's velocity is about 60 m/s. Although the error is only about 6% of the flight distance in the earth centered phase, it is more than 30% of the radius of the lunar gravity influence zone in the moon centered phase. The precision of results will be very low if ignoring the influence of the moon's non-circular orbit [13]. To provide an accurate solution, the moon's position and velocity at any time are obtained by using ephemeris DE405 during the calculation employing the patched-conic method in this section.

Based on this, all the trans-lunar orbit parameters can be denoted as the function of the design variables, which is shown in eq. (1). The detailed formulas are presented in ref. [11].

$$Y_i = f_i(T_B, i_E, u_A, \lambda_B, \varphi_B). \tag{1}$$

c) Constraints.

Different from unmanned lunar exploration, more constraints should be considered in orbit design for manned lunar mission, which contains engineering constraints and orbit constraints.

1) Engineering constraints.

The engineering constraints mainly include flying time constraints and delta velocity (Δv) constraints. Limited by the capability of the spacecraft, the trans-lunar time t_1 and return time t_2 can not be too long, and the TLI Δv_A and LOI Δv_C are also restricted. They should satisfy

$$\begin{cases} t_1 \leqslant T_{1\max}, \quad t_2 \leqslant T_{2\max}, \\ \Delta v_A + \Delta v_C \leqslant \Delta V_{\max}, \end{cases} \tag{2}$$

where $T_{\max}$ is the allowed longest flight time, and $\Delta V_{\max}$ is the maximum delta velocity which can be afforded by propulsion system.

2) Orbit constraints.

The orbit constraints in the earth centered phase, moon centered phase and return phase should be given for FRO design.

Firstly, to economize the fuel consumption, the trans-lunar orbit in the earth centered phase should be elliptic, so the constraint for the eccentricity is

$$e_E < 1. \tag{3}$$

In addition, there are two arriving modes for trans-lunar orbit, long-distance approach and short-distance approach. For the long-distance approach, the flight time from LEO to the entrance point is more than half of the elliptic orbit period, and the true anomaly f_B of spacecraft at the entrance point B satisfies $f_B>\pi$. Otherwise, $f_B<\pi$. The relation between Δv and transfer time in different arriving modes is shown in Figure 3.

Figure 3 shows that the earth-moon transfer time increases with the increasing Δv for the long-distance approach orbit, and that the transfer time is more than 5 days. It is not an optimal orbit for manned lunar mission. Hence, only the short-distance approach orbit is used for manned mission, and the true anomaly of spacecraft at the entrance point B is constrained by

$$f_B < \pi. \tag{4}$$

Secondly, if the spacecraft can be captured by the moon and becomes a lunar satellite when it enters the influence

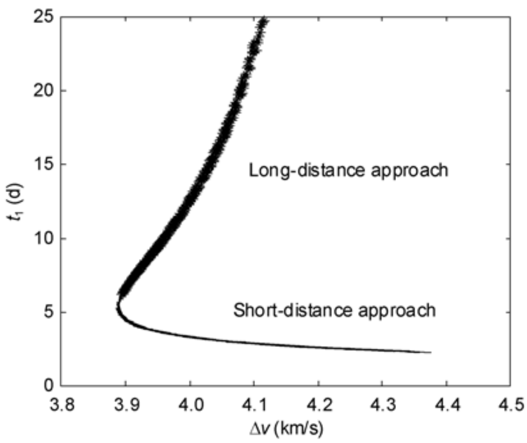

Figure 3 The relationship between transfer Δv and transfer time in different arriving modes.

zone of the lunar gravity, the angle ε should satisfy

$$\varepsilon < \pi / 2, \tag{5}$$

where ε is the angle between the velocity vector $\boldsymbol{v}_B^L$ and the opposite direction of the position vector $\boldsymbol{r}_B^L$, which are shown in Figure 4.

Limited by the altitude of LLO, the perilune altitude of the trans-lunar orbit should be greater than that of the LLO, but not far away from the moon. It is restricted by

$$h_{LP\min} \leqslant h_{LP} \leqslant h_{LP\max}, \tag{6}$$

where h_{LP} is the perilune altitude of FRO, $h_{LP\min}$ and $h_{LP\max}$ are the boundaries of h_{LP}.

Finally, the reentry parameters of the FRO should be constrained for manned lunar mission. The return perigee altitude h_{EP} of the FRO should be lower than the aerosphere boundary, which is

$$0 \leqslant h_{EP} \leqslant 122 \text{ km}. \tag{7}$$

The reentry angle γ_P, which is the angle between velocity vector and horizon, is restricted by the reentry corridor. Here is

$$-10^\circ \leqslant \gamma_P \leqslant -5^\circ. \tag{8}$$

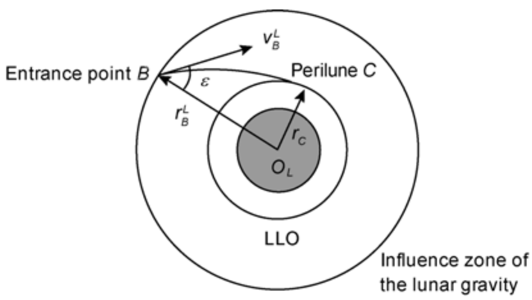

Figure 4 The spacecraft's moon centered orbit parameters.

Eqs. (2)–(8) compose the constraints of the optimal control problem for initial orbit design.

d) Objectives.

Different objectives can be adopted for the optimization problem according to the design missions. Three different objectives are given in this paper.

1) No objective.

No objective is needed if the requirement of the FRO design is only to obtain the orbit parameters that satisfy the above constraints. The optimization problem is converted to nonlinear equations subject to input constraints.

2) Objectives are Δv or the transfer time.

Economizing the fuel consumption or decreasing the transfer time for manned lunar mission is often expected in engineering. Thus, the Δv and transfer time t can be used as objectives for the optimization, which is denoted as

$$J = f(\Delta v, t). \tag{9}$$

3) Objectives are orbit parameters.

Because of the limitation of some engineering conditions for manned lunar mission, morn constraints should always be considered for FRO design, such as the LLO inclination i_L, longitude of ascending node Ω_L, return inclination i_{ER} and so on. These parameters are often fixed according to the engineering conditions and mission object in advance. The FRO design should match these constraints. However, due to the complexity of the nonlinear optimization problem, it is difficult to solve if regarding these parameters as the equation constraints of the optimization. We can convert these equation constraints to the objectives for the optimization problem solution. The objectives is expressed as

$$J = \sum_{i=1}^{n} k_i \left| \delta_i - \delta_{i0} \right|, \tag{10}$$

where δ_i is the actual orbit parameters, δ_{i0} is the desired orbit parameters, k_i is the design weights, and k_i=0 denotes that this orbit parameter is not constrained. When J=0, all the equation constraints are satisfied.

e) Solution algorithm.

Many methods can be used to solve the nonlinear optimization problem, such as the steepest descent algorithm, hill-climbing algorithm, evolution algorithm, particle swarm optimization (PSO), sequential quadratic programming (SQP) and so on. In this section, PSO is employed to solve the optimization problem due to its special search mechanism, the excellent convergence performance and the convenience to realize by computer.

The PSO model introduced by Kennedy and Eberhart in 1995, was discovered through simulation of a simplified social model such as fish schooling or bird flocking. PSO consists of a group of particles moving in the search space. Each particle keeps track of its coordinates in the problem space which are associated with the best solution it has achieved so far. The fitness value is also stored. This value is called *pbest*. Another "best" value that is tracked by the particle swarm optimizer is the best value, obtained so far by any particle in the neighbors of the particle. When a particle takes all the population as its topological neighbors, the best value is a global best and is called *gbest* [14].

For example, the i-th particle is represented as $\boldsymbol{X}_i = (x_{i1}, x_{i2}, \cdots, x_{id})^{\mathrm{T}}$ in the D-dimensional space. The best previous position of the i-th particle is recorded and represented as $\boldsymbol{P}_i = (p_{i1}, p_{i2}, \cdots, p_{id})^{\mathrm{T}}$. The index of the best particle among all the particles in the population is represented by the $\boldsymbol{g}$. The velocity for i-th particle is represented as $\boldsymbol{V}_i = (v_{i1}, v_{i2}, \cdots, v_{id})^{\mathrm{T}}$. The particles are manipulated according to the following equations.

$$\begin{aligned} \boldsymbol{V}_i(t+1) &= \omega \boldsymbol{V}_i(t) + c_1 r_1 (\boldsymbol{P}_i(t) - \boldsymbol{X}_i(t)) \\ &\quad + c_2 r_2 (\boldsymbol{g}(t) - \boldsymbol{X}_i(t)), \\ \boldsymbol{X}_i(t+1) &= \boldsymbol{X}_i(t) + \boldsymbol{V}_i(t+1), \end{aligned} \tag{11}$$

where ω is called the inertia weight and is employed to control the impact of the previous history of velocities on the current one, c_1 and c_2 are acceleration constants, r_1 and r_2 are uniform random numbers drawn from $U(0,1)$.

By employing PSO, the initial parameters of FRO which satisfy the constraints and objectives can be solved effectively.

3.2 Accurate orbit design

A high precision orbit dynamics model under various perturbations is established to obtain the accurate orbit parameters in this section, where the orbit parameters calculated in double two-body model are used as initial design values for accurate optimization solution. SQP is employed to solve the optimization problem which is formulated in the following.

a) Design variables.

The idea for initial orbit design is a converse solution. The orbit parameters in the earth centered phase and moon centered phase are calculated by the orbit parameters given at entrance point. But different from this, a sequence solving idea is used in the accurate orbit design, for which the earth leaving orbit parameters are given, and other parameters are calculated by them. So the design variables for the accurate orbit design are the earth leaving orbit parameters, which contain leaving time T_A, delta velocity Δv_A, leaving LEO inclination i_E, right ascension of ascending node (RAAN) Ω_E and argument of latitude u_E in the ECI coordinate system.

b) Orbit model.

Besides the gravitation of the center body, various perturbations are considered in the high precision orbit dynamics model. The earth centered perturbed equation of motion is established for accurate orbit design, as shown in eq. (12). The orbit parameters of the spacecraft at anytime can be calculated by trajectory integral based on equation [11].

$$\frac{\mathrm{d}^2 \boldsymbol{R}}{\mathrm{d}t^2} = -\frac{\mu_E}{R^2}\frac{\boldsymbol{R}}{R} + \boldsymbol{A}_N + \boldsymbol{A}_{NSE} + \boldsymbol{A}_{NSL} + \boldsymbol{A}_R + \boldsymbol{A}_D, \tag{12}$$

where R is the position vector of the spacecraft in the ECI coordinate system, A_N is the N-body perturbation, A_{NSE} is the nonspherical perturbation of the earth, A_{NSL} is the nonspherical perturbation of the moon, A_R is the solar-radiation pressure perturbation, and A_D is the atmospheric drag perturbation.

c) Constraints and objectives.

The concept of influence zone of the lunar gravity is not used in the accurate orbit design, so the constraints of entrance parameters are not needed here. The primary constraints for the optimization problem in the accurate design are perilune altitude, reentry conditions and engineering requirements. Moreover, the objectives for the optimization problem are the same as that proposed in initial orbit design.

d) Solution algorithm.

SQP algorithm is employed to solve the proposed optimization problem for accurate orbit design. SQP is one of the most popular and robust algorithms for nonlinear optimization. The method is based on solving a series of subproblems designed to minimize a quadratic model of the objective subject to a linearization of the constraints. It is widely used to solve nonlinear programming problems, so we will not give the description in this paper.

However, this algorithm is always sensitive to initial guess. It is difficult to converge or converge to local solutions if the initial control profile is far away from the optimum. Thus, we use the results obtained in initial orbit design as the initial guess of accurate orbit optimization. The result indicates that the calculation is converged quickly in this optimization strategy.

4 Simulation example

In this section, a simulation example is given to validate the FRO design method. The initial conditions and constraints are given as follows. The objectives are ignored.

The time when the spacecraft arrives at the entrance point B: 2025.2.26 0:00;

Inclination of initial LEO: 43°;

Altitude of initial LEO: 334 km;

Constraint of perilune altitude: 110 km–4000 km;

Constraint of return perigee altitude: 0–122 km;

Constraint of reentry angle: −10°– −5°.

The initial FRO parameters, which contain the earth leaving time T_A, delta velocity Δv_A, arriving LLO parameters and return orbit parameters, can be obtained by the using the initial orbit design method. Based on these results, a more accurate FRO is designed by using high precision dynamics model. Table 1 shows the comparison between the initial and accurate design results. Figure 5 shows the flying

Table 1 Comparison between the initial and accurate design results

Orbit model	T_A	i_E	Ω_E	Δv_A	i_L	h_{LP}	i_{ER}	h_{EP}	Total flight time
Double two-body model	2025.2.23	43°	343.897°	3.1125 km/s	175.960°	985.780 km	45.874°	47.400 km	5.8497 d
High precision dynamics model	15:5:1.25		344.211°	3.1139 km/s	175.268°	985.749 km	45.003°	47.492 km	5.8329 d

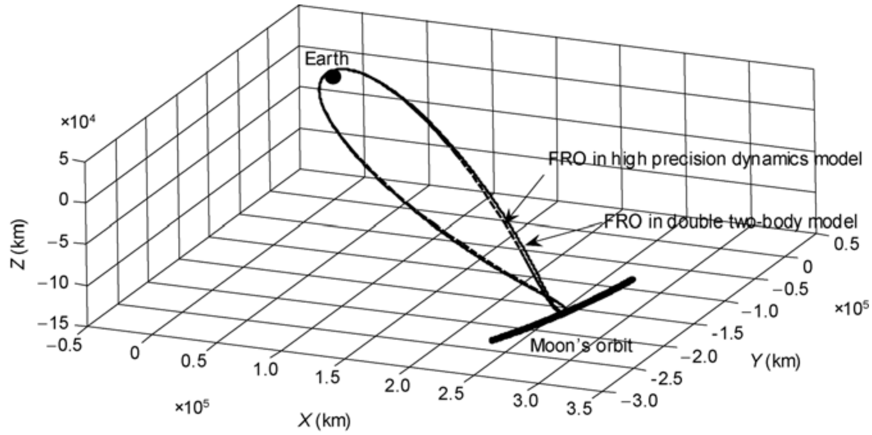

Figure 5 The flying tracks of spacecraft in different design models.

tracks in different design models.

The calculation will be converged quickly in this method. Only about 30 s is needed for one orbit design while calculating by matlab in the PC with a CPU of 3.0 GHz/Pentium 4. So it can be used for orbit characteristics analysis based on population experiments.

The simulation results indicate that the initial orbit parameters also have good precision, and the error with accurate results is very small. At the initial stage of manned lunar mission, the single orbit design is always not concerned in engineering, and the orbit characteristics are more significant. As the initial design results also have good precision, we can only use this model for orbit characteristics analysis, and more calculation time would be saved. Within the improvement of the mission, the high precision model can be employed for accurate orbit design if needed.

5 Orbit characteristics analysis

Based on the above orbit optimization design method, a great deal of simulation experiments are carried out, and the FRO characteristics, which are significant to contrive an orbit scheme for manned lunar mission, are analyzed detailedly in this section.

5.1 Analysis of accessibility of lunar orbit parameters

If a coplanar transfer is required for manned lunar landing from LLO to lunar surface, the LLO should pass the landing site on the moon. In this instance, the choice of lunar landing site is directly affected by the accessible lunar orbit parameters of FRO. Taking the initial conditions and constraints given in the above section as an example, a great deal of FROs satisfied constraints are designed, and the statistic results of accessible lunar orbit parameters are given.

1) Analysis of the range of lunar landing site.

Figure 6 shows the relationship between accessible LLO inclination i_L and longitude of ascending node Ω_L in the MCI coordinate system.

Transforming the MCI into MCF coordinate system, the coverage range of the LLO on lunar surface, which is also the allowed landing site, is shown in Figure 7.

As seen from these two figures, all the accessible LLOs are converse, with $160° < i_L < 180°$. The latitude of landing site is in the range of −26°–26°. So the spacecraft can not arrive anywhere of the lunar surface for FRO. This is the same as the analysis results in Apollo program. The FRO was utilized in Apollo 11 and Apollo 12 missions, so the lunar landing sites for the two missions were near the equator.

2) Primary influencing factors on lunar landing site choice

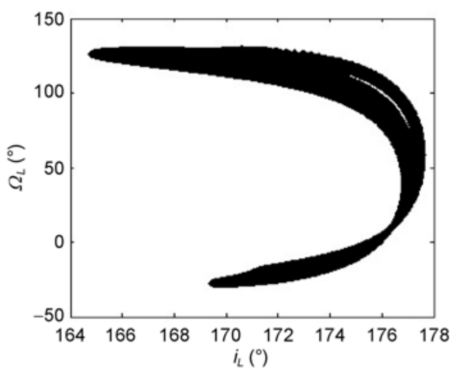

Figure 6 Relationship between LLO inclination i_L and longitude of ascending node Ω_L.

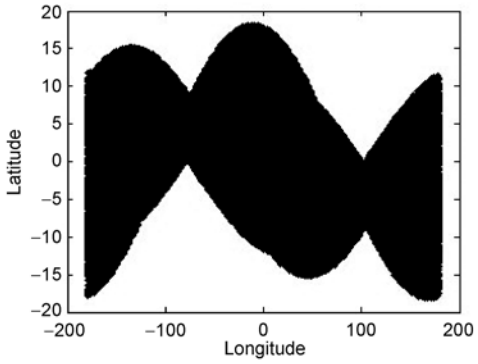

Figure 7 Range of the lunar landing site.

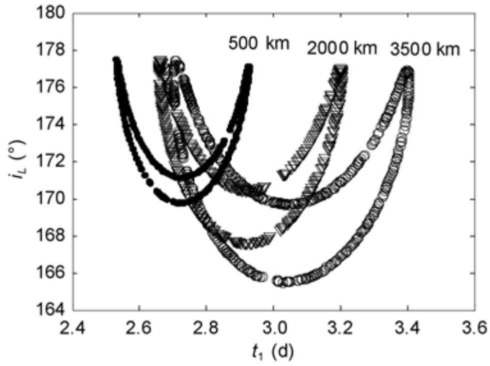

Figure 9 Given h_{LP}, the resulting i_L with respect to t_1.

The accessible range of LLO inclination i_L is also restricted by perilune altitude h_{LP}. Figure 8 shows the accessible range of i_L under different values of h_{LP}.

Figure 8 shows that the accessible range of i_L is increasing as h_{LP} increases, and the spacecraft can get to high latitude area of the moon only in large h_{LP}. For example, the latitude of lunar landing site is 15°, the h_{LP} of FRO should be greater than 3500 km.

In addition, the accessible i_L relates to the trans-lunar time t_1 when h_{LP} is fixed. The relationship between t_1 and i_L under various h_{LP} is shown in Figure 9.

Figure 9 shows that while h_{LP} is fixed, the spacecraft can reach two different LLOs within the same trans-lunar time, for which i_L is different, and the relation curve between t_1 and i_L is approximately a parabola. As seen from Figure 9, the accessible range of i_L is also increasing as h_{LP} increases, which is the same as the above analysis.

5.2 Analysis of earth return orbit parameters

1) Range of the earth return orbit parameters.

The perigee altitude of the return orbit is restricted below the aerosphere boundary, so we merely discuss the inclination i_{ER} and RAAN Ω_{ER} of the return orbit. Figure 10 shows the value of Ω_{ER} corresponding to i_{ER} when the spacecraft reaches the reentry point.

It can be seen that i_{ER} is in the range of 18°–160°, which

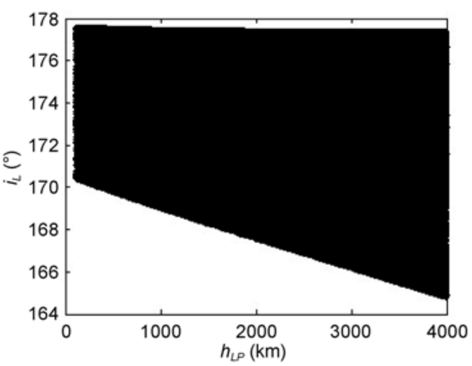

Figure 8 Accessible range of i_L under different h_{LP}.

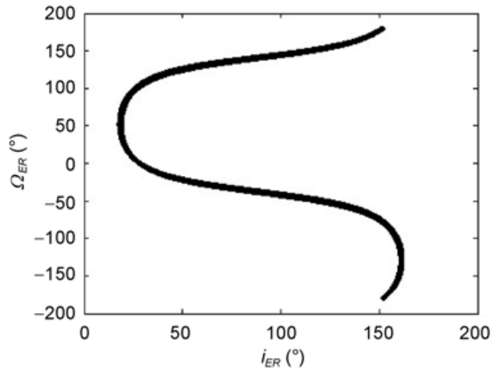

Figure 10 Relation of return orbit RAAN Ω_{ER} with inclination i_{ER}.

has a little change with the moon's position related to the earth, while Ω_{ER} is in the range of −180°–180°. Moreover, there are two different FROs with symmetric Ω_{ER} corresponding to the same i_{ER}. And the relationship between i_{ER} and Ω_{ER} is irrespective to other orbit parameters expect the earth leaving time T_A. Thus, the range of the earth return orbit parameters for FRO can be confirmed with a fixed T_A.

2) Primary influencing factors on return orbit inclination.

According to the above analysis, if the earth leaving time and return orbit inclination are fixed, all of the return orbit parameters are fixed. Therefore, it is of significance for engineering to analyze the primary influencing factors on return orbit inclination.

Figure 11 shows the relationship between i_{ER} and h_{LP} under different trans-lunar times t_1, and Figure 12 shows the relationship between i_{ER} and t_1 under different perilune altitudes h_{LP}.

Figures 11 and 12 illustrate that while the earth leaving time T_A is fixed, there are two FROs satisfying constraints corresponding to the same i_{ER}. In addition, i_{ER} increases as h_{LP} increases, and decreases as t_1 increases.

5.3 Analysis of trans-lunar total Δv

The simulation results indicate that the value of trans-lunar delta velocity Δv is mostly affected by the trans-lunar time t_1 and perigee altitude h_{LP}. Figure 13 shows the change of

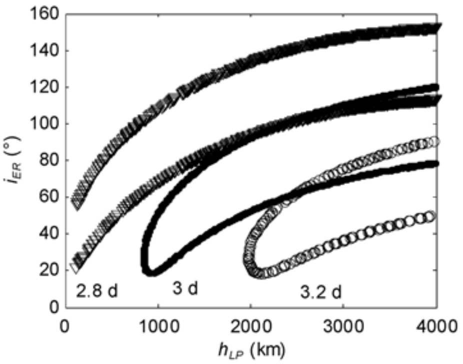

Figure 11 Given t_1, the resulting i_{ER} with respect to h_{LP}.

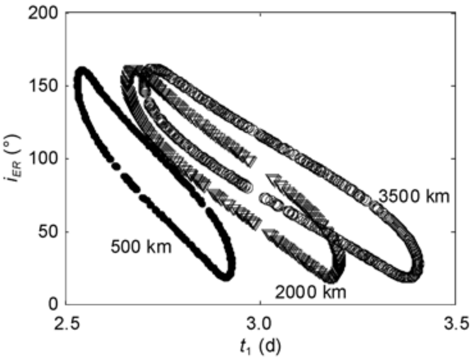

Figure 12 Given h_{LP}, the resulting i_{ER} with respect to t_1.

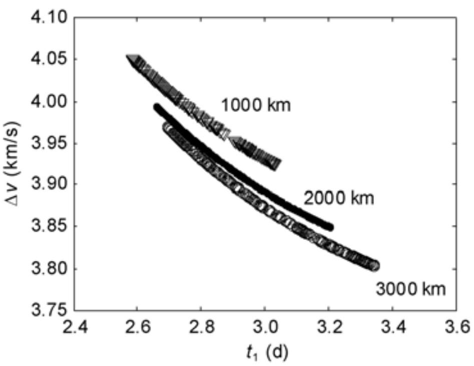

Figure 13 The variation of trans-lunar Δv with trans-lunar time t_1.

Δv with respect to t_1 under different values of h_{LP}.

Figure 13 shows that Δv increases with the increasing t_1 or h_{LP}, and the range of t_1 becomes smaller with the decreasing h_{LP}. For example, if h_{LP}=1000 km, the trans-lunar time can only be in the range of 2.6–3 d.

6 Conclusion

In this paper, by employing optimization algorithm, a serial FRO design strategy from initial value design to accurate solution is proposed. The solution indicates that the calculated FRO can satisfy all the input constraints for manned lunar mission, and that the method has good convergence performance and high accuracy. Based on this, a great deal of FROs are designed, and then its characteristics are analyzed detailedly. The encouraging results have provided significant references for orbit scheme for manned lunar mission.

This work was supported by the National Natural Science Foundation of China (Grant No. 10902121).

1 Berry R L. Launch window and translunar orbit, lunar orbit, and transearth trajectory planning and control for the Apollo 11 lunar landing mission. In: AIAA 8th Aerospace Sciences Meeting, AIAA 70-0024. New York: AIAA, 1970
2 Caldwell S F, Mummert V S. Apollo free return reentry point analysis. NASA-CR-78347, 1966
3 Dupont A L, Bell J A, Alexander J D. Preliminary abort and rescue procedures for Apollo mission F. NASA-TM-X-69838, 1969
4 Beksinski E D. Abort trajectory for manned lunar missions. Dissertation of Masteral Degree. Maryland: Unversity of Maryland, 2007
5 Battin R H. An Introduction to the Mathematics and Methods of Astrodynamics. Reston: American Institute of Aeronautics and Astronautics, Inc., 1999
6 Huang W D, Xi X N, Wang W, et al. Characteristic analysis and design of free return orbit for manned lunar landing based on the double two-body model (in Chinese). J Astron, 2010, 31: 1297–1303
7 Liu X L, Dun G R. Designs of optimal free-return orbit for moon landing. In: Proceedings of the 2007 IEEE International Conference on Robotics and Biomimetics. Sanya: IEEE, 2007. 936–940
8 Zhang L, Yu D Y, Zhang H. Design and analysis of circumlunar free return orbit (in Chinese). Spacecraft Eng, 2010, 19: 128–135
9 Jesick M, Ocampo C. Automated generation of symmetric lunar free-return trajectories. J Guid, Contr, Dynam, 2011, 34: 98–106
10 Luo Y Z, Tang G J, Lei Y J, et al. Optimization of multiple-impulse, multiple-revolution, rendezvous-phasing maneuvers. J Guid, Contr, Dynam, 2007, 30: 946–952
11 Xi X N, Zeng G Q, Ren X, et al. Orbit Design of Lunar Probe (in Chinese). Beijing: National Defense Industry Press, 2001. 51–130
12 Liu L, Wang X. An Orbital Dynamics of Lunar Probe (in Chinese). Beijing: National Defense Industry Press, 2006. 15–50
13 Huang W D, Xi X N, Wang W. Characteristic analysis and design of hybrid trajectory for manned lunar landing mission based on double two-body model (in Chinese). J Nat U Def Tech, 2010, 32: 61–67
14 Li Z J, Liu X D, Duan X D. Simulation on particle swarm optimization for space locus problem (in Chinese). J Sys Simul, 2009, 21: 6086–6090